Graphene Oxides for Homogeneous Dispersion of Carbon Nanotubes

Leilei Tian, Mohammed J. Meziani, Fushen Lu, Chang Yi Kong,[†] Li Cao, Tim J. Thorne, and Ya-Ping Sun*

Department of Chemistry and Laboratory for Emerging Materials and Technology, Clemson University, Clemson, South Carolina 29634-0973, United States

ABSTRACT Graphene oxides (GOs) in terms of both structure and property are essentially polyelectrolytes in a two-dimensional sheet configuration. As is well-established in the literature, polyelectrolytes are, in general, good dispersion agents for single-walled carbon nanotubes (SWNTs), which are otherwise in bundles because of strong van der Waals interactions. We report here a study in which GOs were used to disperse SWNTs, both as-purified and separated semiconducting SWNTs, for solution-like homogeneous suspensions. As a demonstration for their potentials, the optically transparent dispersions were used in a more accurate determination of the absorptivities for the band-gap transitions in semiconducting SWNTs. Results on exploration of the use of the GO-dispersed SWNTs in the development of unique carbon nanocomposite materials are also presented and discussed.

KEYWORDS: graphene oxide • graphene • carbon nanotubes • dispersion • absorptivity • nanocomposite coating

INTRODUCTION

Graphene nanosheets and related materials have attracted considerable recent attention (1−3). In the preparation for graphene nanosheets, the route of using exfoliated graphene oxides (GOs) as precursors has been widely pursued (4, 5). GOs are typically obtained by processing graphite under extreme oxidative conditions (in the Hummers method, in particular) (6, 7). With the oxidation and associated introduction of oxygen-containing groups, a significant portion of the graphene π-electronic network is destroyed in the formation of GOs. As a result, exfoliated GOs are readily dispersed in water to form essentially an aqueous solution (7, 8).

Structural and propertywise GOs resemble polyelectrolytes in a two-dimensional sheet configuration. Their surfactant-like characteristics at interfaces have also been reported recently (9). As was already established in the literature, polyelectrolytes play a valuable role in the development and study of carbon nanomaterials, especially in the dispersion of single-walled carbon nanotubes (SWNTs), which are otherwise in bundles because of strong intertube van der Waals interactions (10−12). As derivatized carbon nanomaterials themselves, GOs with their polyelectrolyte properties may serve as a special class of dispersion agents for carbon nanotubes (in fact, during the preparation of this manuscript, a study on the dispersion of multiple-walled carbon nanotubes by GOs was reported (13)). This is valuable to more quantitative investigations of the nanotubes and to the development of unique carbon nanocomposite materials (14). Here we report a study in which GOs were used to disperse SWNTs, both as-purified and separated semiconducting SWNTs, for solution-like suspensions, which made it possible to determine quantitatively the optical absorption parameters of SWNTs. Results that demonstrate significant potentials of the GO-dispersed SWNTs in the development of unique carbon nanocomposite materials are also presented and discussed.

RESULTS AND DISCUSSION

GOs were prepared from a commercially supplied graphite sample by using the Hummers method with minor modification (6). The as-prepared sample was dispersed in water for further exfoliation via sonication, followed by high-field (14 000*g*) centrifugation to keep the supernatant as an aqueous suspension of well-exfoliated GOs (15). The GOs thus obtained were in the acid form because of the oxidation of carbons at graphene sheet edges and defects in carboxylic acids (16). They were converted to the salt form (similar to the "sodium form" in other polyelectrolytes such as Nafion polymers) (17, 18) in order to make their aqueous dispersion more stable (15). The GO samples in the solid state were characterized by Raman spectroscopy, from which the results suggested no meaningful differences between the acid and salt forms. The Raman G- and D-band features for both samples were similar to those already reported in the literature (19). In this study, GOs in the salt form were used throughout all subsequent experiments (though GOs in the acid form could also be used for the same purpose). As shown in Figure 1, the aqueous suspended GOs at neutral pH appeared solution-like and optically transparent, with the color varying from light yellow to brownish depending on the concentration (but no absorption contributions beyond 500 nm) (20). Electron microscopy images of GO pieces are shown in Figure 2.

* To whom correspondence should be addressed. E-mail: syaping@clemson.edu.

Received for review August 3, 2010 and accepted September 24, 2010

[†] On leave from Department of Materials Science and Chemical Engineering, Faculty of Engineering, Shizuoka University, 3-5-1 Johoku, Naka-ku, Hamamatsu 432-8561, Japan.

DOI: 10.1021/am100687n

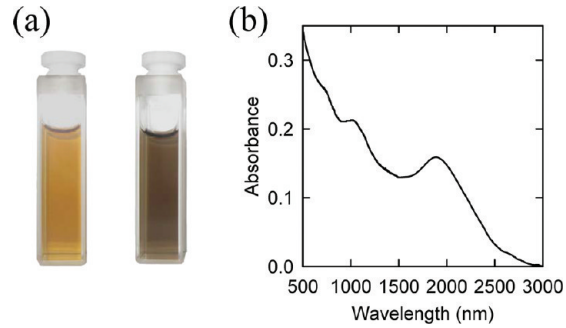

FIGURE 1. (a) Photographs for aqueous GOs without (left) and with dispersed SWNTs (right). (b) Optical absorption spectrum of a film on glass from the dispersion with a GO/SWNT weight ratio of unity.

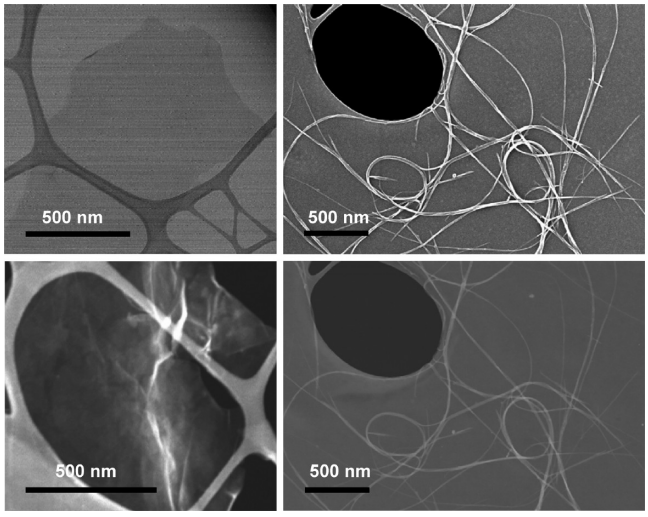

FIGURE 2. TEM images (upper, transmission mode; lower, Z-contrast mode) of GO pieces (left) and purified SWNTs (right).

The aqueous GOs were found to be highly effective in the dispersion of purified SWNTs, where the GOs play the role of a potent polyelectrolyte. In a typical experiment, a weighed amount of the specially purified SWNTs (with the purity in terms of the sample volume reaching 99 %; Figure 2) (21) was added to the aqueous GOs, and the mixture was sonicated until a visually homogeneous dispersion was formed. Upon settling, the sediment, if any, was collected and analyzed. It was found that when the weight ratio between GOs and SWNTs to be dispersed was ≥ 1, the SWNTs were dispersed quantitatively (in the sense of all nanotubes dispersed, not necessarily at the individual nanotube level) (22−24) by the aqueous GOs without any residues (Figure 1).

The aqueous GO-dispersed SWNTs were used to cast optically transparent thin films. The absorption spectrum of a carefully dried (under vacuum at ambient temperature) film is shown in Figure 1, which is featured by the characteristic transitions associated with the van Hove singularity pairs in the electronic density of states in semiconducting (S_{11} and S_{22} peaks at 1920 and 1025 cm^{-1}, respectively) and metallic (M_{11} at 720 cm^{-1}) SWNTs (25).

The same films described above were characterized by resonance Raman spectroscopy (632.8 nm excitation) and scanning electron microscopy (SEM). In the Raman spectra of GOs and SWNTs separately for reference and comparison,

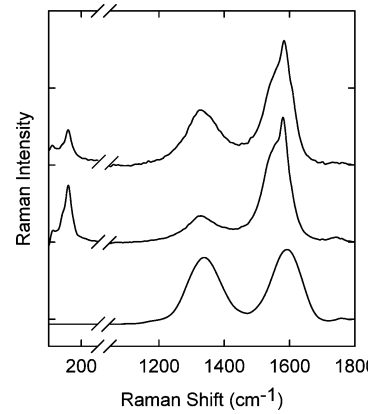

FIGURE 3. Raman spectra of GOs (lower), pure SWNTs (middle), and a GO-SWNT composite with a weight ratio of unity (upper).

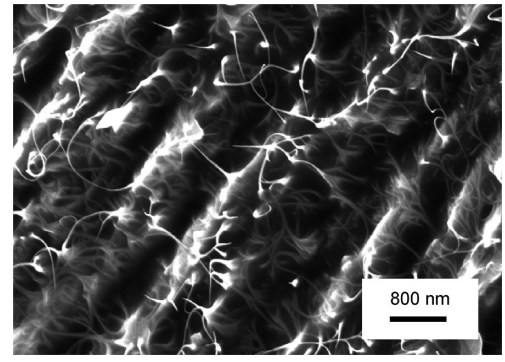

FIGURE 4. Representative SEM image on the fracture edge of a film prepared from aqueous GO-dispersed SWNTs.

the G band of GOs was broader and symmetric, and the D band was understandably more intense (Figure 3) (19). However, in resonance Raman spectra of the composite films, the G band was obviously dominated by SWNTs (Figure 3) because no absorption for GOs at the excitation wavelength and thus no resonance enhancement occurred. On the other hand, the D band in the films was disproportionally higher, probably because of both the contribution of GOs and the effects similar to those observed in the functionalization of SWNTs. The radial breathing mode of SWNTs was shifted slightly to a higher frequency (Figure 3), consistent with the nanotubes being "sandwiched" between GOs. For SEM evaluation, the films were fractured on purpose. Shown in Figure 4 is a typical SEM image on the fracture edge of a film. The results are rather similar to those found for well-dispersed or functionalized SWNTs in polymeric nanocomposite films (26).

The suspension was also diluted and deposited onto a holey carbon-coated copper grid for transmission electron microscopy (TEM) analyses. While probing for detailed information on the dispersion of SWNTs by GOs at the nanoscale was not successful likely because of a lack of sufficient contrast between the species (Figure 5), individual SWNTs were found under high-resolution TEM conditions (Figure 5).

The aqueous dispersions of GO-dispersed SWNTs were homogeneous and optically transparent (Figure 1), enabling quantitative optical absorption measurements under solution-like conditions. Shown in Figure 6 are observed absorp-

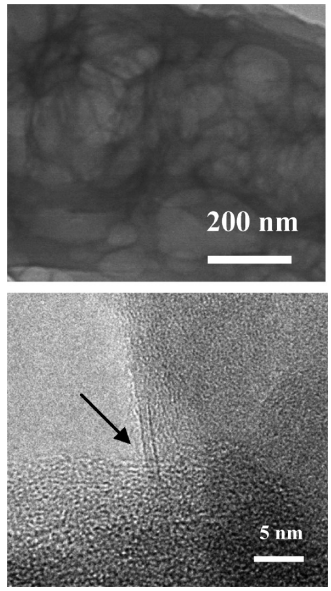

FIGURE 5. TEM images obtained at different resolutions for the specimen prepared from deposition of a few drops of a dilute suspension of GO-dispersed SWNTs onto a holey carbon-coated copper grid and then drying.

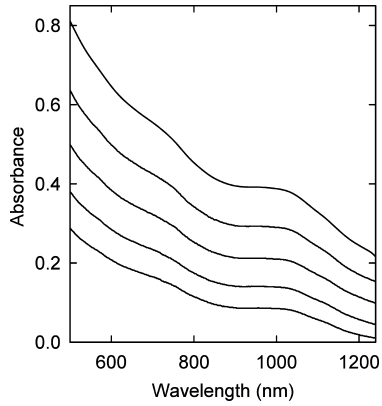

FIGURE 6. As-measured optical absorption spectra of aqueous GO-dispersed pure SWNTs at increasing nanotube concentrations (mg/L, from lower to upper): 13, 16, 19, 23, and 28.

tion spectra in the 500−1250 nm spectral region because GOs had no absorption contributions at longer than 500 nm, and water absorption became overwhelming beyond 1250 nm (making it impossible to record the S_{11} band). By keeping the amount of GOs constant, the concentration of SWNTs was varied such that the highest corresponded to the GOs-to-SWNTs ratio of unity, thus ensuring quantitative dispersion of SWNTs by GOs throughout variation in the nanotube concentrations. As shown in Figure 7, there was a proportional dependence of the S_{22} peak absorbance on the nanotube concentration. Under the assumption that no background correction was necessary, as a first approximation, this proportional dependence would coincide with the Beer's law plot, from which an absorptivity value of ~21.5 $(g/L)^{-1}$ cm^{-1} at the S_{22} band maximum was obtained. This agrees with the value reported by Haddon and co-workers from the measurement of similar arc-discharge SWNTs suspended in *N*,*N*-dimethylformamide (DMF) (27), but at the lower end of a wide range of values [up to 35 $(g/L)^{-1}$ cm^{-1}] available in the literature (28−30). Because DMF is known as an excellent solvent for the relatively more homogeneous dispersion of SWNTs, the agreement between this work and that of Haddon and co-workers does suggest that GOs are effective dispersion agents for SWNTs in aqueous solution.

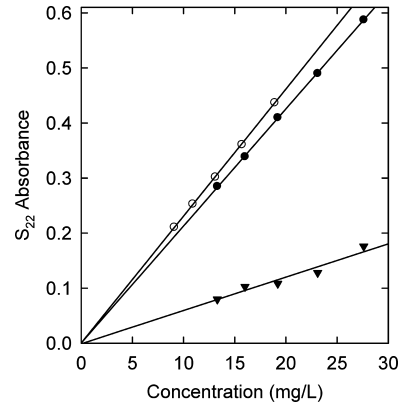

FIGURE 7. Beer's law plots for the peak absorbance of the S_{22} band in as-measured spectra of aqueous GO-dispersed pure SWNTs (●) and the separated semiconducting SWNTs (○) and in the background-corrected absorption spectra (▼).

For the aqueous GO-dispersed SWNTs, the GOs had no absorption contributions in the concerned spectral region (longer than 500 nm), as discussed above, so no background correction due to GOs in the dispersions was necessary. Nevertheless, the presence of other background absorptions, especially the widely considered π-plasmon absorption (31, 32), was likely. In fact, various theoretically driven correction schemes for π-plasmon and other background absorptions have been proposed and practiced in a number of studies (28, 29, 33). A shortcoming of those correction schemes was their heavy reliance on the validity of the largely simplified theoretical descriptions in such complicated systems (nanotubes of different lengths and other properties). Thus, in this study, we were looking for a correction scheme based only on experimentally determined absorption parameters. Our correction took advantage of the availability of separated semiconducting SWNTs (largely free from metallic SWNTs).

It is already established in the literature that as-produced SWNTs are generally mixtures of metallic and semiconducting nanotubes, with a ratio of 1:2 in samples from arc-discharge production used in this study. In unrelated studies reported previously (34−36), a postproduction separation method exploiting selective interactions of large planar aromatic molecules with semiconducting SWNTs was developed (35−37). The available separated semiconducting sample (containing more than 95% semiconducting SWNTs) was used in this study for the same dispersion by GOs. The resulting homogeneous dispersions were also solution-like, hardly distinguishable from those of the purified SWNTs without separation. Optical absorption measurements of the dispersions yielded a similarly proportional relationship of the absorbance with the nanotube concentration, except for a higher slope (Figure 7). At the S_{22} band and other long wavelengths (no absorption contributions from metallic SWNTs), the ratio of observed absorbances for the separated semiconducting sample against the sample without separa-

tion at the same nanotube concentration should be close to 3:2 because in the latter the content of the semiconducting SWNTs is only 2:3. Thus,

$$[(A_{semi})_{obs} - A_{back}]/[(A_{mix})_{obs} - A_{back}] = 3:2 \qquad (1)$$

where $(A_{semi})_{obs}$ is the observed absorbance for the semiconducting SWNT sample, $(A_{mix})_{obs}$ the observed absorbance for the mixture, and A_{back} the background absorption to be corrected. Obviously, eq 1 allows calculation of A_{back} from the experimental $(A_{semi})_{obs}$ and $(A_{mix})_{obs}$ data. Upon background correction, the true Beer's law plot for the S_{22} absorption peak in the aqueous GO-dispersed SWNTs is also shown in Figure 7, where the slope corresponds to an average S_{22} peak absorptivity of 6 $(g/L)^{-1}$ cm^{-1}. This is larger than the value of 3.8 $(g/L)^{-1}$ cm^{-1} reported by Haddon and co-workers for arc-discharge-produced SWNTs in a DMF suspension, for which the estimate was based on the assumption of a linear relationship (on the wavenumber scale) for the absorption background (28). An even smaller value of 2.2 $(g/L)^{-1}$ cm^{-1} was reported by Sun and co-workers for the same SWNTs functionalized with aminopoly(ethylene glycol) oligomers (PEG_{1500N}) in a carbon disulfide (CS_2) solution, for which the background correction was also based on a rough approximation (38).

The S_{11} band could not be measured in the aqueous environment because of overwhelming water absorption. In thin films, it is safe to eliminate the offset (primarily due to scattering) to set the absorbance to zero at 3000 nm (beyond the onset of S_{11} absorption; Figure 1). According to Haddon and co-workers (28), the absorption background correction should be made on the wavenumber scale (proportional to energy). By using their assumption of a linear background (zero at 3000 nm or 3330 cm^{-1}; Figure 1) and also maximal background correction until no negative absorbance over the spectral region for S_{11} and S_{22} bands (28), the estimated S_{11}-to-S_{22} peak absorbance ratio was about 2. This would thus correspond to a S_{11} peak absorptivity of about 12 $(g/L)^{-1}$ cm^{-1} under the further assumption of no meaningful differences between solution-phase and solid-state absorptivities. In the literature, results on the S_{11} absorptivity were surprisingly scarce, with only the report by Sun and co-workers for arc-discharge-produced SWNTs functionalized with PEG_{1500N} in a CS_2 solution (38). The S_{11}-to-S_{22} peak absorbance ratio found in that study was 2.2, similar to the roughly estimated value here, although the S_{11} and S_{22} peak absorptivity values in the PEG_{1500N}-functionalized SWNTs were both smaller (38).

The optical absorptivities of SWNTs (S_{11} and S_{22}) are important electronic transition parameters. The use of aqueous GOs for the homogeneous nanotube dispersion and the availability of separated semiconducting SWNTs in this work made it possible to avoid some of the rough approximations necessary in previous studies, so that the absorptivity values reported here should be more accurate. It was a concern that the GOs as dispersion agents would potentially have significant doping effects on especially the S_{11} absorption. However, this was not supported by the results because the S_{11}-to-S_{22} ratio thus determined was not so different from that obtained previously under different experimental conditions (38), and the S_{11} and S_{22} peak absorptivity values were both larger than those found in previous studies. Regarding the absorptivity, the S_{11} peak value on a per mole of carbon basis is ~144 $[M(carbon)]^{-1}$ cm^{-1}, smaller than the per carbon molar absorptivities in common small planar aromatic molecules, such as ~570 $[M(carbon)]^{-1}$ cm^{-1} in anthracene. This suggests relatively weaker but still substantial transitions for these near-IR electronic band gaps in semiconducting SWNTs.

The more accurate determination of the optical absorption parameters of SWNTs is just one example for the utility of the homogeneously dispersed nanotubes by aqueous GOs. The effective dispersion also enables the use as precursors of all-carbon nanocomposite materials that retain significant optical transparency. These materials have been widely pursued for their superior electrical, thermal, and/or other properties. For example, SWNTs with their high electrical conductivity are investigated extensively in the development of next-generation transparent conductive electrodes (36, 39−41), which represent the core component in a variety of optoelectronic devices and systems. As reported in the literature, surfactants such as sodium dodecyl sulfate (SDS) are commonly used in the dispersion of SWNTs for subsequent wet-casting of transparent conductive films at ambient temperature. The large amount of the surfactant used for the nanotube dispersion must be removed postfabrication, which could prove challenging, while the morphology of the nanotube films must be maintained or controlled to ensure the desired electrical conductive properties (42).

In this work, the aqueous GO-dispersed SWNTs were wet-casted into ultrathin optically transparent films on a glass substrate (typically 75 mm × 25 mm; Figure 8). For an as-fabricated film (GO-dispersed SWNTs) of 85% transmittance at 550 nm, the observed surface resistivity was ~4 kΩ/□, lower than those of the similarly fabricated films with the same optical transmittance at 550 nm from DMF-suspended SWNTs (>20 kΩ/□) and the SDS-assisted dispersion of SWNTs (~5 kΩ/□ even after careful removal of SDS postfabrication). The surface morphology of the film was examined by SEM. As is also shown in Figure 8, the nanotubes were apparently dispersed without any phase separation (from GOs) or substantial aggregation.

In the optically transparent films from aqueous GO-dispersed SWNTs (Figure 8), removal of GOs would not be necessary because GOs are widely used as precursors for graphene nanosheets, which like SWNTs have been recently pursued as new carbon nanomaterials for potentially revolutionary applications in transparent conductive electrodes (43−45). Such a prospect highlights the unique advantage of the use of GOs in the homogeneous dispersion of SWNTs for optically transparent all-carbon nanocomposite materials/devices and beyond. Investigations to exploit such a unique advantage are in progress, and the results will be reported in due course.

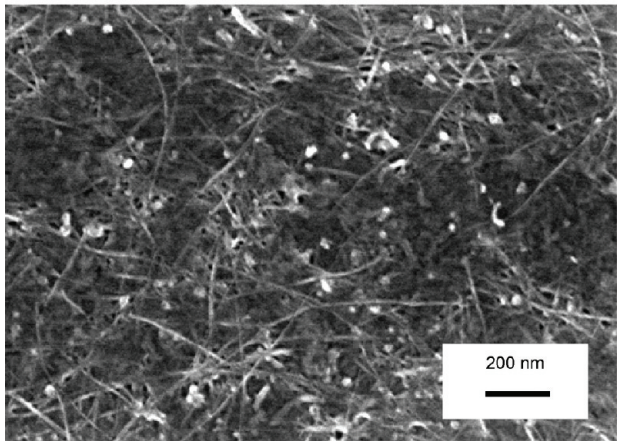

FIGURE 8. Upper: Photographs of transparent conductive coatings on a glass substrate (left to right: 95%, 85%, and 78% optical transmittance at 550 nm), fabricated by a simple air-spray method from aqueous GO-dispersed pure SWNTs. Lower: SEM image on the surface morphology of the film in the middle.

In summary, the reported results suggest that GOs are highly effective in the dispersion of SWNTs to form optically transparent solution-like aqueous suspensions. As a demonstration for their valuable applications, the homogeneous dispersions were used for a more accurate determination of absorptivities for the band-gap transitions in semiconducting SWNTs. The use of aqueous GO-dispersed SWNTs in the fabrication of transparent conductive coatings, though preliminary, has already achieved significant performance (~4 kΩ/□ for 85% transmittance at 550 nm, with only simple air-spray fabrication) and will be further explored in continuing investigations.

EXPERIMENTAL SECTION

Materials. The arc-discharge-produced sample of SWNTs ("AP-SWNT", carbonaceous purity 40−60%) was supplied by Carbon Solutions, Inc., and the graphite sample (surface-enhanced flake graphite, grade 3805) by Asbury Carbons. Sulfuric acid (93%), nitric acid (73%), hydrochloric acid (36%), hydrogen peroxide (35%), and phosphorus pentoxide (P_2O_5) were obtained from Acros, ammonium persulfate [$(NH_4)_2S_2O_8$] was obtained from Aldrich, and potassium permanganate ($KMnO_4$) was obtained from Fisher Scientific. Poly(vinylidene difluoride) membrane filters (0.22 μm pore size) were purchased from Fisher Scientific, the dialysis membrane tubing (MWCO ~ 3500) was purchased from Spectrum Laboratories, and carbon-coated copper grids were purchased from SPI Supplies. Water was deionized and purified by being passed through a Labconco WaterPros water purification system.

Graphene Oxides (GOs). The Hummers method (6) with minor modification was used for the preparation of GOs from graphite. Briefly, to the concentrated H_2SO_4 (10 mL) in a flask at 80 °C were added $(NH_4)_2S_2O_8$ (0.9 g) and P_2O_5 (0.9 g), and the mixture was stirred until the reagents were completely dissolved. Graphite (1 g) was added, and the resulting mixture was allowed to react at 80 °C for 4.5 h. Upon being cooled to room temperature, the reaction mixture was diluted with water (250 mL) and kept for ~12 h. It was then filtered and washed repeatedly with water, followed by drying in a vacuum oven. The solid sample was added to concentrated H_2SO_4 (40 mL) in a flask cooled in an ice bath. To the mixture in the flask was added slowly $KMnO_4$ (5 g over 40 min), during which the temperature was kept at <10 °C. The resulting mixture, with a change in color from black to greenish-brown, was heated at 35 °C for 2 h, followed by dilution with water (85 mL; ***Caution!*** *the temperature must be kept at <35 °C throughout!*) and further stirring for 2 h. The reaction mixture was poured into a large beaker, to which water (250 mL) and then aqueous H_2O_2 (30%, 10 mL) were added. Bubbles from the aqueous mixture along with a color change to brilliant yellow were observed. The mixture was allowed to settle for ~12 h. The clear supernatant was decanted, and the sediment was washed repeatedly with an aqueous H_2SO_4 (5 wt %), H_2O_2 (0.5 wt %), and HCl (10 wt %) solution, followed by washing repeatedly with water until no layers were observed in the centrifugation. The sample was then dialyzed (MWCO ~ 3500) against water for 7 days to yield a clean aqueous dispersion of GOs.

The as-prepared GOs (acid form) in an aqueous suspension were titrated with an aqueous NaOH solution (0.1 M) until pH 9 (for GOs in the sodium form), followed by dialysis (MWCO ~ 3500) against water for 7 days. The GOs in an aqueous suspension (~0.2 wt %) were further exfoliated via sonication for 30 min. The resulting brown-colored suspension was centrifuged at 14 000*g* for 30 min to retain the supernatant (containing about 80% of the starting sample) as aqueous dispersed GOs (sodium form).

SWNTs: Purification and Separation. The as-supplied sample of SWNTs was purified in two steps: the widely used method with nitric acid treatment and, subsequently, further purification based on reversible noncovalent functionalization by 1-pyreneacetic acid, as reported previously (21). The purity of the nanotube sample was at least 95% by weight and higher by volume (because the residual metal catalysts are much higher in density than that of carbon).

Separation of the purified SWNTs into metallic and semiconducting fractions was based on a well-developed method already patented (37) and reported with detailed procedures in the literature (35, 36). The separated sample used in this study contained at least 95 wt % of semiconducting SWNTs.

Dispersion. Aqueous GOs were used to disperse SWNTs. In a typical experiment, the purified sample of SWNTs (1−10 mg) was added to the aqueous GOs (0.02 wt %, 25 mL), and the mixture was sonicated until a visually homogeneous dispersion was formed. Upon settling for 24 h, the sediment, if any, was collected and analyzed. It was found that when the amount of starting nanotube sample to be dispersed was small (5 mg or less), the SWNTs could be dispersed quantitatively by the aqueous GOs without any residues.

The same experimental procedures and conditions were used for dispersion of the separated semiconducting SWNTs by aqueous GOs.

Measurements. A bath sonicator (VWR model 950DA), a homogenizer (PowerGen 125), and a benchtop centrifuge (Eppendorf model 5417R) were used in the purification, dispersion, and other procedures. Optical absorption spectra were recorded on a Shimadzu UV-3600 UV/vis/near-IR spectrophotometer. Raman spectra were obtained on a Jobin Yvon T64000 Raman spectrometer equipped with a Melles-Griot He−Ne laser source (35 mW) for 632.8 nm excitation, a triple monochromator, a liquid-nitrogen-cooled symphony detector, and an attached Olympus BX-41 microscope for sampling. SEM imaging was performed on a Hitachi S4800 field-emission SEM system, and TEM analyses were carried out on Hitachi 9500 and Hitachi HD-2000 TEM systems.

The aqueous GO-dispersed SWNTs were simply spray-cast onto a glass substrate for ultrathin films of various optical transparencies. The electrical current (I) and voltage (V) relationships for the films were determined by using the traditional four-probe method. The setup included a multimeter (Keithley 2400, controlled by Lab Tracer 2.0 software, both from Keithley Instruments) and a multiheight probe (Jandel). The surface resistivity values for the films were calculated as $R_s = (\pi/\ln 2)(I/V)$.

Acknowledgment. This work was made possible by financial support from the Air Force Office of Scientific Research (AFOSR) through the program of Dr. Charles Lee. M.J.M. was supported by the American Chemical Society Petroleum Research Fund. C.Y.K. was supported by the Excellent Young Researchers Overseas Visit Program of Japan Society for the Promotion of Science. L.C. was supported by a Susan G. Komen for the Cure Postdoctoral Fellowship. T.J.T. was a participant in the Palmetto Academy, an education-training program managed by the South Carolina Space Grant Consortium.

REFERENCES AND NOTES

(1) Geim, A. K.; Novoselov, K. S. *Nat. Mater.* **2007**, *6*, 183.
(2) Rao, C. N. R.; Sood, A. K.; Subrahmanyam, K. S.; Govindaraj, A. *Angew. Chem., Int. Ed.* **2009**, *48*, 7752.
(3) Allen, M. J.; Tung, V. C.; Kaner, R. B. *Chem. Rev.* **2010**, *110*, 132.
(4) Dreyer, D. R.; Park, S.; Bielawski, C. W.; Ruoff, R. S. *Chem. Soc. Rev.* **2010**, *39*, 228.
(5) Compton, O. C.; Nguyen, S. T. *Small* **2010**, *6*, 711.
(6) Hummers, W.; Offeman, R. E. *J. Am. Chem. Soc.* **1958**, *80*, 1339.
(7) Stankovich, S.; Dikin, D. A.; Piner, R. D.; Kohlhaas, K. A.; Kleinhammes, A.; Jia, Y.; Wu, Y.; Nguyen, S. T.; Ruoff, R. S. *Carbon* **2007**, *45*, 1558.
(8) Szabo, T.; Berkesi, O.; Forgo, P.; Josepovits, K.; Sanakis, Y.; Petridis, D.; Dekany, I. *Chem. Mater.* **2006**, *18*, 2740.
(9) Kim, J.; Cote, L. J.; Kim, F.; Yuan, W.; Shull, K. R.; Huang, J. *J. Am. Chem. Soc.* **2010**, *132*, 8180.
(10) Zheng, M.; Jagota, A.; Semke, E. D.; Diner, B. A.; Mclean, R. S.; Lustig, S. R.; Richardson, R. E.; Tassi, N. G. *Nat. Mater.* **2003**, *2*, 338.
(11) Sinani, V. A.; Gheith, M. K.; Yaroslavov, A. A.; Rakhnyanskaya, A. A.; Sun, K.; Mamedov, A. A.; Wicksted, J. P.; Kotov, N. A. *J. Am. Chem. Soc.* **2005**, *127*, 3463.
(12) Paloniemi, H.; Aaritalo, T.; Laiho, T.; Liuke, H.; Kocharova, N.; Haapakka, K.; Terzi, F.; Seeber, R.; Lukkari, J. *J. Phys. Chem. B* **2005**, *109*, 8634.
(13) Zhang, C.; Ren, L.; Wang, X.; Liu, T. *J. Phys. Chem. C* **2010**, *114*, 11435.
(14) Dikin, D. A.; Stankovich, S.; Zimney, E. J.; Piner, R. D.; Dommett, G. H. B.; Evmenenko, G.; Nguyen, S. T.; Ruoff, R. S. *Nature* **2007**, *448*, 457.
(15) Li, D.; Muller, M. B.; Gilje, S.; Kaner, R. B.; Wallace, G. G. *Nat. Nanotechnol.* **2008**, *3*, 101.
(16) Xu, Y. X.; Zhao, L.; Bai, H.; Hong, W. J.; Li, C.; Shi, G. Q. *J. Am. Chem. Soc.* **2009**, *13*, 13490.
(17) Young, R. J. *Introduction to Polymers*; Chapman and Hall: New York, 1983; p 204.
(18) Mauritz, K. A.; Moore, R. B. *Chem. Rev.* **2004**, *104*, 4535.
(19) Kudin, K. N.; Ozbas, B.; Schniepp, H. C.; Prud'homme, R. K.; Aksay, I. A.; Car, R. *Nano Lett.* **2008**, *8*, 36.
(20) Paredes, J. I.; Villar-Rodil, S.; Martinez-Alonso, A.; Tascon, J. M. D. *Langmuir* **2008**, *24*, 10560.
(21) Lu, F.; Xin, W.; Meziani, M. J.; Cao, L.; Tian, L. L.; Bloodgood, M. A.; Robinson, J.; Sun, Y.-P. *Langmuir* **2010**, *26*, 7561.
(22) Fagan, J. A.; Landi, B. J.; Mandelbaum, I.; Simpson, J. R.; Bajpai, V.; Bauer, B. J.; Migler, K.; Hight Walker, A. R.; Raffaelle, R.; Hobbie, E. K. *J. Phys. Chem. B* **2006**, *110*, 23801.
(23) Zhou, B.; Lin, Y.; Hill, D. E.; Wang, W.; Veca, L. M.; Qu, L.; Pathak, P.; Meziani, M. J.; Diaz, J.; Connell, J. W.; Watson, K. A.; Allard, L. F.; Sun, Y.-P. *Polymer* **2006**, *47*, 5323.
(24) Lacerda, L.; Pastorin, G.; Wu, W.; Prato, M.; Bianco, A.; Kostarelos, K. *Adv. Funct. Mater.* **2006**, *16*, 1839.
(25) Hamon, M. A.; Itkis, M. E.; Niyogi, S.; Alvaraez, T.; Kuper, C.; Menon, M.; Haddon, R. C. *J. Am. Chem. Soc.* **2001**, *123*, 11292.
(26) Lin, Y.; Meziani, M. J.; Sun, Y.-P. *J. Mater. Chem.* **2007**, *17*, 1143.
(27) Bekyarova, E.; Itkis, M. E.; Cabrera, N.; Zhao, B.; Yu, A. P.; Gao, J. B.; Haddon, R. C. *J. Am. Chem. Soc.* **2005**, *127*, 5990.
(28) Zhao, B.; Itkis, M. E.; Niyogi, S.; Hu, H.; Zhang, J.; Haddon, R. C. *J. Phys. Chem. B* **2004**, *108*, 8136.
(29) Landi, B. J.; Ruf, H. J.; Evans, C. M.; Cress, C. D.; Raffaelle, R. P. *J. Phys. Chem. B* **2005**, *109*, 9952.
(30) Jeong, S. H.; Kim, K. K.; Jeong, S. J.; An, K. H.; Lee, S. H.; Lee, Y. H. *Synth. Met.* **2007**, *157*, 570.
(31) Shyu, F. L.; Lin, M. F. *Phys. Rev. B* **1999**, *60*, 14434.
(32) Lauret, J. S.; Voisin, C.; Cassabois, G.; Delalande, C.; Roussignol, P.; Jost, O.; Capes, L. *Phys. Rev. Lett.* **2003**, *90*, 057404.
(33) Itkis, M. E.; Perea, D. E.; Niyogi, S.; Rickard, S. M.; Hamon, M. A.; Zhao, B.; Haddon, R. C. *Nano Lett.* **2003**, *3*, 309.
(34) Chattopadhyay, D.; Galeska, I.; Papadimitrakopoulos, F. *J. Am. Chem. Soc.* **2003**, *125*, 3370.
(35) Li, H. P.; Zhou, B.; Lin, Y.; Gu, L. R.; Wang, W.; Fernando, K. A. S.; Kumar, S.; Allard, L. F.; Sun, Y.-P. *J. Am. Chem. Soc.* **2004**, *126*, 1014.
(36) Wang, W.; Fernando, K. A. S.; Lin, Y.; Meziani, M. J.; Veca, L. M.; Cao, L.; Zhang, P.; Kimani, M. M.; Sun, Y.-P. *J. Am. Chem. Soc.* **2008**, *130*, 1415.
(37) Sun, Y.-P. On Process for Separating Metallic from Semiconducting Single-Walled Carbon Nanotubes. U.S. Patent 7,374,685.
(38) Zhou, B.; Lin, Y.; Li, H. P.; Huang, W. J.; Connell, J. W.; Allard, L. F.; Sun, Y.-P. *J. Phys. Chem. B* **2003**, *107*, 13588.
(39) Bekyarova, E.; Itkis, M. E.; Cabrera, N.; Zhao, B.; Yu, A. P.; Gao, J. B.; Haddon, R. C. *J. Am. Chem. Soc.* **2005**, *127*, 5990.
(40) Zhang, D. H.; Ryu, K.; Liu, X. L.; Polikarpov, E.; Ly, J.; Tompson, M. E.; Zhou, C. W. *Nano Lett.* **2006**, *6*, 1880.
(41) Geng, H. Z.; Kim, K. K.; So, K. P.; Lee, Y. S.; Chang, Y.; Lee, Y. H. *J. Am. Chem. Soc.* **2007**, *129*, 7758.
(42) Geng, H. Z.; Lee, D. S.; Kim, K. K.; Han, G. H.; Park, H. K.; Lee, Y. H. *Chem. Phys. Lett.* **2008**, *455*, 275.
(43) Becerril, H. A.; Mao, J.; Liu, Z.; Stoltenberg, R. M.; Bao, Z.; Chen, Y. *ACS Nano* **2008**, *2*, 463.
(44) Wang, X.; Zhi, L. J.; Müllen, K. *Nano Lett.* **2008**, *8*, 323.
(45) Shin, H. J.; Kim, K. K.; Benayad, A.; Yoon, S. M.; Park, H. K.; Jung, I. S.; Jin, M. H.; Jeong, H. K.; Kim, J. M.; Choi, J. Y.; Lee, Y. H. *Adv. Funct. Mater.* **2009**, *19*, 1987.

AM100687N